

# **Transverse Polarization Effects in Hard Scattering at CLAS**

H. Avakian, V. Burkert, L. Elouadrhiri  
Jefferson Lab, Newport News, VA 23606

K. Griffioen  
The College of William and Mary, Williamsburg, 23187-8795

B. Seitz  
Univ. of Glasgow, Glasgow G12 8QQ, UK

M. Garçon and F. Sabatié  
DAPNIA/SPhN, CEA-Saclay, F-91191 Gif-sur-Yvette, France

K. Joo  
University of Connecticut, Physics Department, Storrs, CT 06269, USA

D. Crabb, C. Smith  
University of Virginia, Charlottesville, VA 22903

V. Kubarovsky, P. Stoler  
Rensselaer Polytechnic Institute, Troy, NY 12181, USA

## Abstract

Electroproduction of final state photons and mesons off the transversely polarized protons using a 11 GeV electron beam and the CLAS12 detector at Jefferson Lab will be used to measure target single-spin asymmetries. Significant azimuthal angle dependent moments were predicted in photon and meson hard exclusive as well as semi-inclusive cross section for a transversely polarized target. Measured transverse-target single-spin asymmetries in combination with the data available from unpolarized and longitudinally polarized targets would allow extraction and separation of different generalized parton distributions and transverse momentum dependent distributions, eventually giving access to the the orbital momentum of partons. This measurement will also provide a simple test of the applicability of GPD based predictions for hard exclusive production of pseudoscalar and vector mesons at JLAB energies.

## 1 Introduction

Deep inelastic scattering (DIS) has been used extensively in recent years as an important testing ground for QCD. Studies so far have been concentrated on better determination of parton distribution functions (PDFs) describing momentum fraction distributions of partons in the infinite momentum frame. The use of polarization in leptonproduction provides an essential new dimension for testing QCD. Polarized quark distributions have been extracted from a combination of inclusive and semi-inclusive asymmetry data [1, 2]

At leading-twist, the quark structure of hadrons is described by three distribution functions: the number density  $q(x)$ ; the helicity distribution  $\Delta q(x)$ , and the transversity distribution  $\delta q(x)$ . Although parton distribution functions cannot be computed in perturbative QCD, they are infact universal and do not depend on the particular hard process. Once measured in semi-inclusive DIS (SIDIS) no extra input is needed in order to compute analogous quantities in hadron-hadron collisions. However as the results from DIS suggest [3], only a fraction of nucleon spin can be attributed to the quark spins. In recent years PDFs were generalized to contain information not only on the longitudinal but also the transverse distributions of partons in a fast moving hadron. Much of the interest in Generalized Parton Distributions (GPDs) [4, 5] has been triggered by their potential to help to unravel spin structure of the nucleon, as they contain information not only on the helicity carried by partons, but also on their orbital angular momentum. The QCD factorization theorem has been generalized to a large group of hard exclusive processes [6],

$$\gamma^*(q) + T(p) \rightarrow \gamma(q') + T'(p'); \quad \gamma^*(q) + T(p) \rightarrow M(q') + T'(p')$$

in which a photon  $\gamma^*$  with high energy and large virtuality  $-q^2 = Q^2 > 0$  scatters off the hadronic target  $T$  and produces a final state photon  $\gamma$  or hadron  $M$ .



distribution functions		chirality	
		even	odd
twist 2	U	<b>q</b>	$h_1^\perp$
	L	<b><math>\Delta\mathbf{q}</math></b>	$h_{1L}^\perp$
	T	$f_{1T}^\perp$ <b><math>g_{1T}</math></b>	$\delta\mathbf{q}$ $h_{1T}^\perp$

Table 1: List of twist-2 TMD distribution functions accessible in SIDIS.

The leading twist GPDs defining the cross section for different final states are termed  $H^q$ ,  $\tilde{H}^q$ ,  $E^q$ , and  $\tilde{E}^q$ , and depend upon three kinematic variables:  $x$ ,  $\xi$ , and  $t$ . The variable  $\xi$  is the longitudinal momentum fraction of the transfer  $\Delta = p' - p$ ,  $t = \Delta^2$  is the overall momentum transfer in the process ( $p$  and  $p'$  are initial and final nucleon momenta). In the forward limit ( $\Delta \rightarrow 0$ ), the GPDs  $H$  and  $\tilde{H}$  reduce to the quark density distribution  $q(x)$  and quark helicity distribution  $\Delta q(x)$  respectively. The functions  $E$  and  $\tilde{E}$  are not measurable through DIS. There is a sum rule [4] that relates the second moment of the quark helicity-independent GPDs to the fraction of the nucleon spin ( $J$ ) carried by the sum of the quark spin and orbital angular momentum:

$$\int_{-1}^1 dx \, x \, (H(x, \xi) + E(x, \xi)) = 2J. \quad (1)$$

Another class of nonperturbative functions that carry information not only on longitudinal but also on transverse hadron structure are transverse momentum dependent (TMD) parton distributions [7, 8]. If the transverse momentum  $k_T$  of partons also included, the number of independent distribution functions at leading twist increases to six [7, 8] (three of which reduce to  $q(x)$ ,  $\Delta q(x)$  and  $\delta q(x)$  when integrated over  $k_T$ ). Because they depend on the longitudinal and transverse momentum, these “3-dimensional” transverse momentum dependent (TMD) functions provide a more complete picture of nucleon structure. Relaxing the time invariance condition, two additional functions ( $f_{1T}^\perp$ ,  $h_1^\perp$ ) are permitted, bringing the total number of distribution functions to eight. The full list of twist-2 distribution functions (those that survive after the  $k_T$ -integration are denoted in boldface) contributing to the double-polarized cross section in SIDIS is shown in Table 1 (see [7]). As shown recently in Ref.[9], the interaction of active parton in the hadron and the target spectators [10, 11, 12] leads to gauge-invariant TMD parton distributions.

The physical picture becomes particularly intuitive after a Fourier transform from transverse momentum transfer to impact parameter, both for GPDs [13, 14] and TMDs [14]. GPDs in impact parameter space or impact parameter dependent (IPD) distributions probe partons at transverse position  $\vec{b}$ . The impact parameter gives the location where a quark or antiquark is pulled out of and put back into the proton. The difference in transverse positions is a *global* shift in each wave function; the *relative*

transverse distances between the partons in a hadron are the same before and after the scattering.

In contrast to GPDs in TMD distributions describing the correlation in transverse position of a single parton, the struck quark has a different transverse location *relative* to the spectator partons in the initial and the final state wave functions, in addition to the overall shift of the proton center of momentum. Both TMDs  $q(x, \mathbf{k}_\perp)$  and IPDs  $q_X(x, \mathbf{b}_\perp)$  are linked to the orbital momentum of partons and lead to predictions of single-spin asymmetries (SSA) in hard scattering processes [15, 44, 7, 8, 16, 13]. It was demonstrated recently that a nonzero orbital angular momentum of partons in the nucleon is crucial in forming the target single-spin asymmetries. Measurement of the azimuthal angle distributions of observed photons and hadrons in hard exclusive and semi-inclusive leptonproduction allows access to both GPDs and TMDs [44, 10, 13].

Large beam SSA were measured in deep exclusive electroproduction of photons (DVCS) both at HERMES [20] and CLAS [21]. HERMES collaboration presented recently first results on transverse target SSA measurements providing a first glimpse of the GPD E and contribution to orbital momentum from  $u$ -quarks [22].

Recently, significant SSAs were reported in semi-inclusive DIS (SIDIS) by the HERMES collaboration at HERA [23, 24, 25] for a longitudinally polarized target, the SMC collaboration at CERN for a transversely polarized hydrogen [26], and the CLAS collaboration at JLab [27, 28] with a polarized beam and target. Single-spin asymmetry measurements in SIDIS opened up a unique possibility to access T-odd distribution functions in semi-inclusive DIS [10, 11]. The flavor dependence of the corresponding functions [31, 32] is the main focus of experiments with 6 GeV electrons at JLab, 27.5 GeV positrons at HERMES and 160 GeV muons at COMPASS, using various polarized and unpolarized targets.

**CLAS12 with a transversely polarized target will allow simultaneous measurement of beam and target SSA of different final state particles including photons (DVCS) and pseudoscalar and vector mesons in a wide range of different kinematic variables.**

## 1.1 Current Fragmentation in SIDIS at 6GeV

Important issues at low beam energies are the separation of current and target fragmentation regions and the presence of factorization when the quark scattering process and the fragmentation process factorize, and the fragmentation functions depend only on the fractional energy,  $z$ . At low beam energies in DIS the current fragmentation region (CFR) is contaminated with events coming from the target fragmentation region (TFR). A nice graphical representation of different regions as a function of relevant kinematic variables  $z$ ,  $x_F$  and  $\eta$  is available from Mulders and collaborators. At low  $z$  and  $x_F$  and rapidities  $\eta < 1$  a significant overlap is expected of current and target fragmentation regions (see Fig. 1).

Factorization in  $z$ -distributions of pions was studied using the the 6 GeV data from

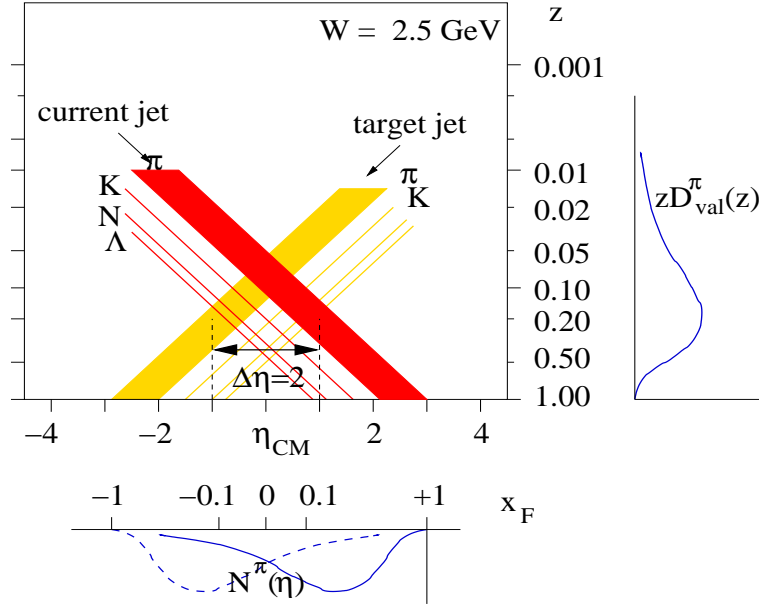


Figure 1: The SIDIS kinematics at  $W = 2.5$  GeV. The kinematic variables are defined as follows:  $z = \frac{E_h}{\nu}$ ,  $x_F = \frac{p_L^*}{p_{Lmax}^*}$  and  $\eta = \frac{1}{2} \ln \frac{E+p_L^*}{E-p_L^*}$ .

CLAS[28] and Hall-C[29] experiments. No significant dependence within statistical uncertainties was observed in  $z$ -distributions for different values of  $x$ .

## 1.2 Transversely polarized target

The preliminary studies are showing that it is technically possible to run a polarized target with CLAS12. In this case the Solenoid magnet and central detector will be removed and replaced by a standalone polarized target, similar to the existing polarized target used in electron scattering experiments. As the magnetic field orientation is transverse to the beam direction the electron beam will be deflected vertically. This will be compensated for by installing a magnetic chicane upstream of the target so that the beam after the target is again in the horizontal plane. Special care is needed for the shielding of electromagnetic background, especially Møller electrons.

There is currently a transverse polarized target under study for use in the 6 GeV program with CLAS in Hall-B. The target concept is such that it can be operated with CLAS12 as well. The target will have a warm bore for the target cryostat that also allows detection of slow protons in specially designed magnetic field insensitive detectors located around the target cryostat.

The kinematic coverage for the transversely polarized target is shown on Fig. 2.

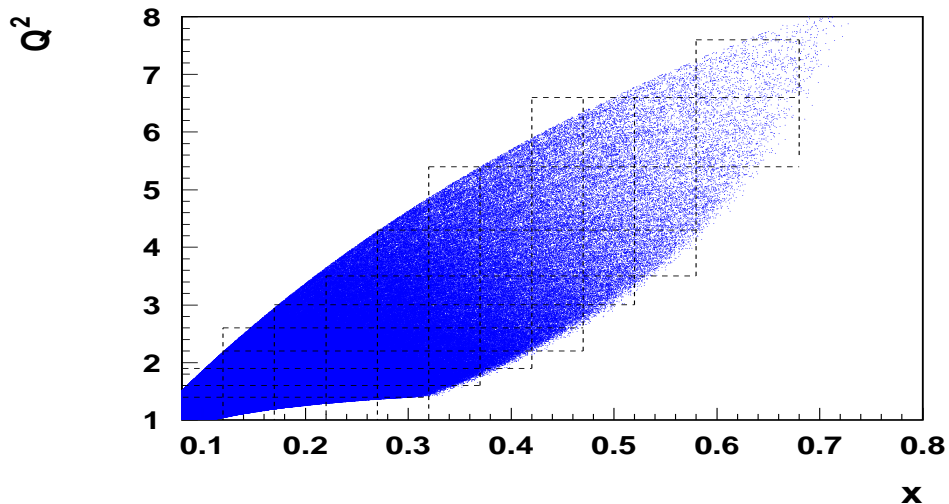


Figure 2: Kinematic coverage with transverse target (electron angles below  $22.5^\circ$ ).

## 2 Semi-Inclusive Pion SSAs

Single-spin asymmetries in SIDIS give access to distribution and fragmentation functions, which cannot easily be accessed in other ways. The list of novel physics observables accessible in SSAs includes the chiral-odd distribution functions, such as the transversity ( $\delta q$ ) [42, 43], the *time-reversal odd* fragmentation functions, in particular the Collins function ( $H_1^\perp$ ) [44], and recently introduced [15, 45, 10, 11, 12] *time-reversal odd* distribution functions ( $f_{1T}^\perp, h_1^\perp$ ).

The SSA in the  $\sin \phi$  moment of the cross section for unpolarized beam and transversely polarized target is defined as:

$$A_{UT}^{\sin \phi} = \frac{\langle \sin \phi \rangle_{UT}}{\langle \sin^2 \phi \rangle_{UT}} = \frac{1}{P^\pm N^\pm} \frac{\sum_{i=1}^{N^\pm} \sin \phi_i}{\sum_{i=1}^{N^\pm} \sin^2 \phi_i}, \quad (2)$$

where  $P^\pm$  and  $N^\pm$  are polarization value and number of events for corresponding polarization state.

A detailed study of  $Q^2$  and  $x_B$  dependencies as a function of the azimuthal angle  $\phi$  will allow the separation of contributions from different mechanisms.

### 2.1 Transversity and Sivers function

The leading twist transversity distribution  $\delta q$  [42, 43] and its first moment, the tensor charge, are as fundamental for understanding of the spin structure of the

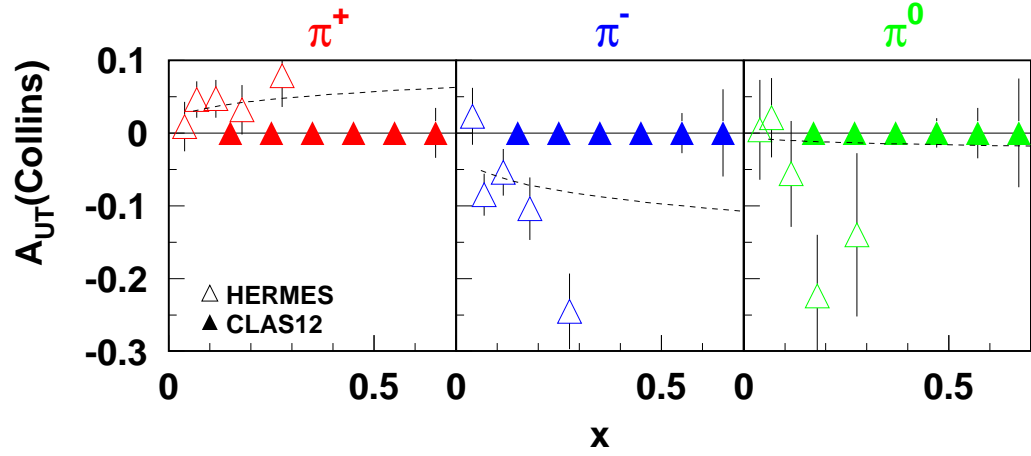


Figure 3: Projected transverse spin asymmetry from the Collins effect ( $A_{UT}^{\sin(\phi+\phi_s)}$ ) in single  $\pi$  production with CLAS at 11 GeV.

nucleon as are the helicity distribution  $\Delta q$  and the axial vector charge. The transversity distribution  $\delta q$  is charge conjugation odd. It does not mix with gluons and for non-relativistic quarks it is equal to the helicity distribution  $\Delta q$ . Thus, it probes the relativistic nature of quarks and it has a very different from  $g_1$   $Q^2$  evolution. Its first moment, tensor charge is reliably calculable in lattice QCD with  $\delta\Sigma = \sum_f \int_0^1 dx (\delta q_f - \delta \bar{q}_f) = 0.562 \pm 0.088$  at  $Q^2 = 2\text{GeV}^2$ , which is twice as large as the value of proton axial charge [47]. A similar quantity ( $\delta\Sigma \approx 0.6$ ) was obtained in the effective chiral quark soliton model [48].

At leading twist, the effect of quark transversity can be measured via the azimuthal asymmetry in fragmentation in SIDIS [44]. For transversely polarized targets, several azimuthal asymmetries already arise at leading order. Four contributions related to corresponding distribution functions were investigated in Refs. [44, 7, 8, 10, 12, 46]:

$$\sigma_{LT}^{\cos\phi} \propto \lambda_e S_T y (1 - y/2) \cos(\phi - \phi_S) \sum_{q,\bar{q}} e_q^2 x g_{1T}^q(x) D_1^q(z), \quad (3)$$

$$\begin{aligned} \sigma_{UT}^{\sin\phi} &\propto S_T (1 - y) \sin(\phi + \phi_S) \sum_{q,\bar{q}} e_q^2 x \delta q(x) H_1^{\perp q}(z), \\ &+ S_T (1 - y + y^2/2) \sin(\phi - \phi_S) \sum_{q,\bar{q}} e_q^2 x f_{1T}^{\perp q}(x) D_1^q(z), \end{aligned} \quad (4)$$

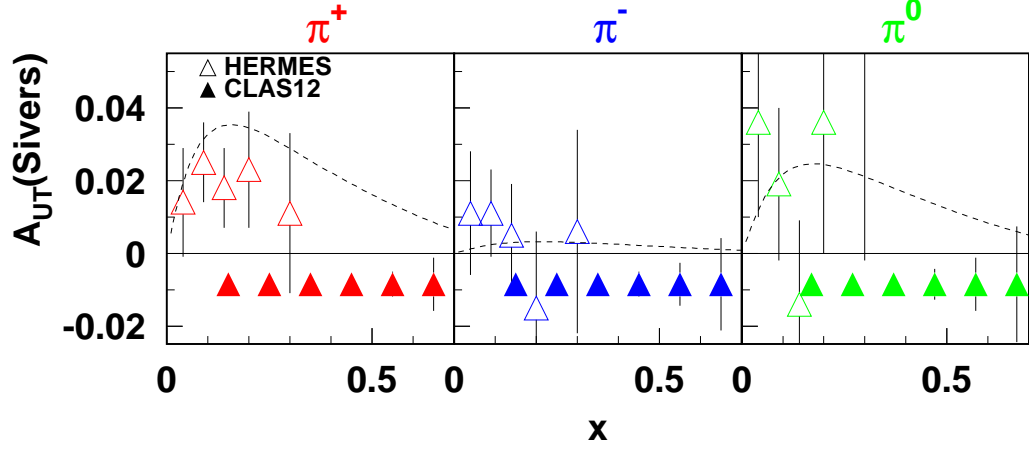


Figure 4: Projected transverse spin asymmetry from the Sivers effect ( $A_{UT}^{\sin(\phi-\phi_S)}$ ) in single  $\pi$  production with CLAS at 11 GeV.

$$+ S_T(1-y)\sin(3\phi-\phi_S)\sum_{q,\bar{q}}e_q^2xh_{1T}^{\perp q}(x)H_1^{\perp q}(z), \quad (5)$$

where  $\phi_S$  is the azimuthal angle of the transverse spin in the photon frame and  $D_1^q(z)$  is the spin-independent fragmentation function.

The first equation for the transversely polarized target describes a double-spin asymmetry giving access to the leading-twist TMD  $g_{1T}^q(x)$  appearing in convolution with the unpolarized fragmentation function  $D_1^q(z)$  in a  $\cos\phi$  moment of the cross section. Significant asymmetries were predicted recently for CLAS12 [53] (see Fig.5) providing access to  $g_{1T}^q(x)$ , describing longitudinally polarized quarks in the transversely polarized nucleon.

The latter three equations describe single-spin asymmetries involving the first moments of T-odd Sivers distribution function and Collins fragmentation function integrated over the transverse momentum of initial and final state quarks correspondingly.

The  $\sin\phi$  moment of the SIDIS cross section (Eq.5) with a transversely polarized target ( $\sigma_{UT}$ ) [49] contains contributions both from the Sivers effect (T-odd distribution convoluted with  $D_1^q(z)$ ) [15] and the Collins effect (T-odd fragmentation convoluted with transversity) [44].

Contributions to transverse SSAs from T-odd distributions of initial quarks ( $f_{1T}^{\perp q}(x)$  term) and T-odd fragmentation of final quarks ( $H_1^{\perp q}(z)$  term) could be sep-

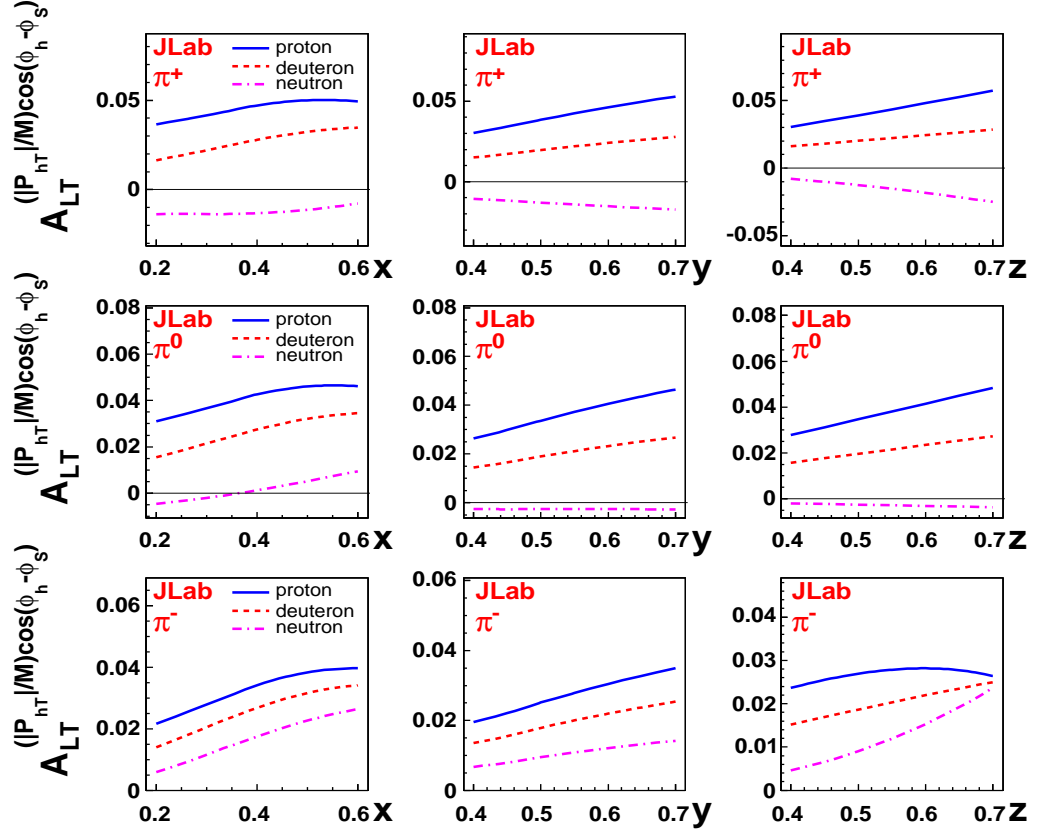


Figure 5: Predictions for the weighted double spin asymmetry  $A_{LT}$  for CLAS at 11 GeV [53]

arated by their different azimuthal and  $z$ -dependences.

The full acceptance coverage in  $\phi$  provides redundancy in the data in that the interdependent spin and spatial asymmetries are measured together. The method of extracting the analyzing power was chosen to exploit this redundancy in a way that simplifies the evaluation of the systematic errors.

Projections for target single-spin asymmetry measurements with CLAS at 11 GeV are plotted in Figs. 3-6. The curves are calculated by Efremov et al for  $z > 0.45$  and the missing mass of the  $e'\pi$  system ( $M_X(\pi^+) > 1.1$  GeV). The projected error bars have been calculated assuming a luminosity of  $5 \times 10^{34} \text{cm}^{-2} \text{s}^{-1}$ , with a  $NH_3$  target polarization of 85% and a dilution factor of 0.14, with 2000 hours of data taking. The asymmetry is integrated over all hadron transverse momenta. The extraction of the transversity from  $A_{UT}^{\sin \phi}$  could be performed using parameterizations for the unpolarized distribution functions  $u(x)$  and  $\bar{d}(x)$ . and certain approximations for the

polarized Collins fragmentation function  $H_1^\perp$ .

The target single-spin asymmetry from polarized quark fragmentation extracted for CLAS12 kinematics at 11 GeV is plotted in Fig. 3. The estimate was done assuming  $\delta q \approx \Delta q$  and an approximation for the Collins fragmentation function from Ref.[50]. Additional cuts were applied on  $z$  ( $z > 0.5$ ) and the missing mass of the  $e'\pi^+$  system ( $M_X(\pi^+) > 1.3$  GeV). The curves have been calculated assuming a luminosity of  $5 \times 10^{34} \text{cm}^{-2} \text{s}^{-1}$ , with a  $NH_3$  target polarization of 85% and a dilution factor 0.14, with 2000 hours of data taking. The asymmetry is integrated over all hadron transverse momenta.

The measurement of transversity is complicated by the presence of an essentially unknown Collins function. Recently, the Collins function for pions was calculated in a chiral invariant approach at a low scale [33] and it was shown that at large  $z$  the function rises much faster than previously predicted [50, 51] in the analysis using the HERMES data on target SSA. It was also pointed out that the ratio of polarized and unpolarized fragmentation is almost scale independent[33]. Significant asymmetry was measured by Belle [38] indicating that the Collins function is indeed large. The transverse asymmetry measurements were performed at HERMES[24] and COMPASS[37]. Significant asymmetry was observed for both Collins and Sivers effects at HERMES [25]. However, the statistics is not enough to extract the corresponding distribution and fragmentation functions.

Significantly higher statistics from CLAS12 data, especially in the large  $x$  region, will enable the extraction of the  $x$  and  $Q^2$  dependencies for different azimuthal moments in a wide kinematical range allowing to reveal the source of the observed SSA and extract underlying distribution functions. The extraction of the Sivers function from 1000 hours of CLAS12 using the  $\pi^0$  production (CLAS12 with IC setup) is shown on Fig. 6.

The measurement of the transverse asymmetry from the Sivers effect (see Fig. 6) with  $\pi^0$  will provide model independent extraction of the Sivers function. Furthermore, measurements with proton and neutron targets will provide a model independent information on flavor partners of the Sivers function.

The wide kinematic coverage of CLAS12 combined with high beam polarization and high luminosity allows precision measurements of semi-inclusive processes in the target fragmentation region (TFR). The TFR corresponds to the backward hemisphere in the CM frame requiring negative values for the Feynman variable,  $x_F$ , defined as a longitudinal fraction of the hadron momentum in CM frame.

Presence of asymmetry in parton distributions due to orbital motion of polarized quarks leading to observed asymmetries in hadronic distributions in current fragmentation [25] will lead to similar asymmetries, but with opposite sign for hadronic distributions in the target fragmentation region. A projection for measurement of Sivers asymmetry in target fragmentation for 2000h of CLAS12 running at luminosity of  $5 \times 10^{34} 1/\text{sec}^{-1} \text{cm}^{-2}$  is shown on Fig. 7. Curves are calculated using an approximation for Sivers function extracted from  $pp$  SSAs [52]



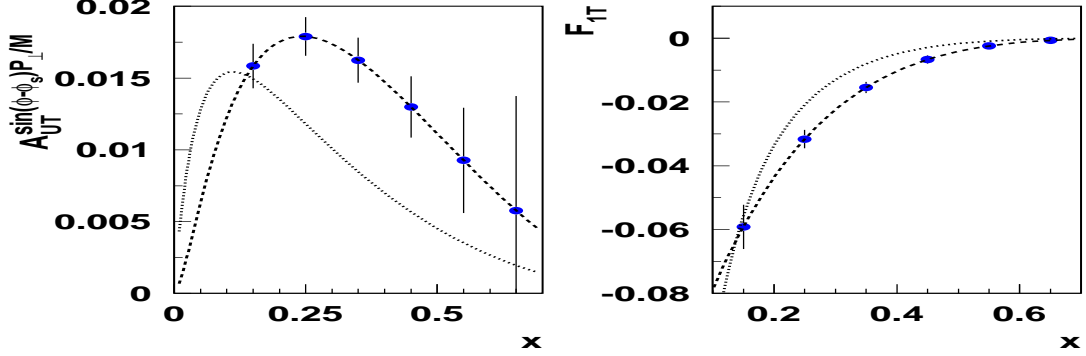


Figure 6: Projected transverse spin asymmetry ( $A_{UT}^{\sin\phi}$ ) in single  $\pi^+$  production with CLAS at 11 GeV.

Measurement of non-zero SSAs in semi-inclusive DIS of pions in target fragmentation region with a transversely polarized target will ensure that measured SSAs at HERMES and CLAS12 with transverse target are driven by the Sivers effect.

### 3 DVCS

The hard electroproduction of real photons (DVCS) is one of the cleanest tools in the problem of constraining GPDs from data. Extraction of GPDs from the DVCS data requires measurements with different target and beam polarizations. First measurements of the DVCS process for unpolarized target most sensitive to the GPD  $H$  was reported by ZEUS [54], H1 [55], HERMES [20] and CLAS [21] collaborations presented the first results on DVCS measurements. The DVCS SSA, with longitudinally polarized target, which is most sensitive to the polarized GPD, was measured for the first time by the CLAS collaboration [57]. HERMES Collaboration presented first results on DVCS SSA both for longitudinal and transverse target polarizations [58],[59]. The DVCS SSA for transversely polarized target is most sensitive observable to the elusive GPD  $E$ , providing access to the orbital angular momentum.

There is a number of theoretical uncertainties in phenomenological predictions for DVCS. Apart from the basically unconstrained shape of GPDs, which one models on the ground of previous theoretical considerations, these are higher-twist and -order effects, which alter the handbag approximation. The former include the dynamical and target mass corrections.

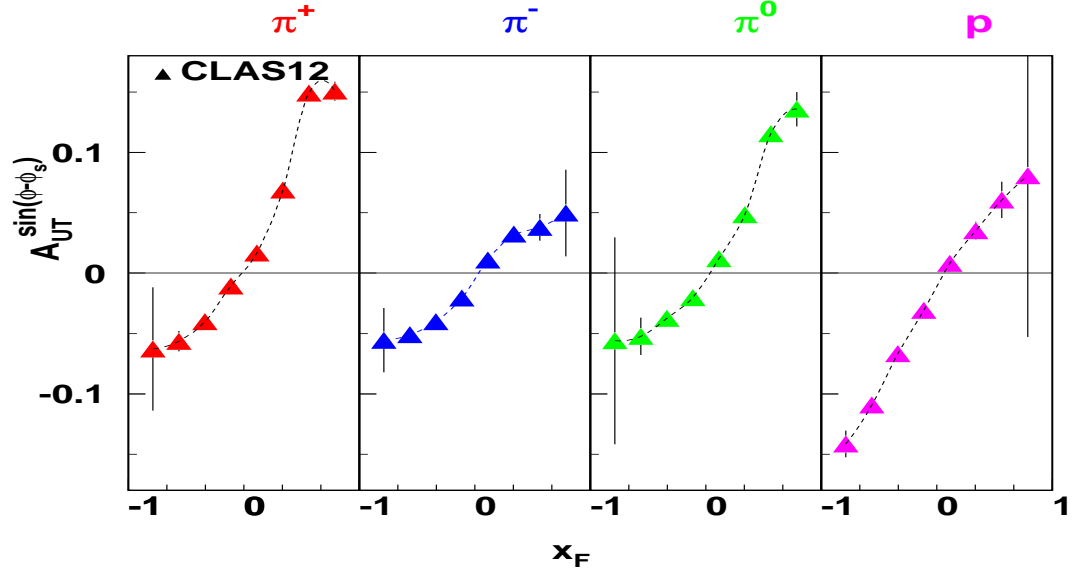


Figure 7: Siverts asymmetry in TFR for different hadrons

Consequences of the target and lepton beam polarizations for accessing the generalized parton distributions from experimental measurements of the azimuthal angular dependence of the final state photon or nucleon was presented in Ref. [56]. Several sets of asymmetries, defined as Fourier moments with respect to the azimuthal angle and which allow for a clear separation of the twist-two and -three sectors, were introduced. The differential lepton production cross section was extensively analyzed with power accuracy for all polarization options of the lepton beam and target. It was pointed out that the most favorable physical observables to unravel GPDs from cross sections are spin-azimuthal asymmetries. These asymmetries allow us to extract separate components of the angular dependence of the cross section and, in this manner, to project out distributions carrying information on the orbital momentum of constituents in the nucleon.

The five-fold cross section for the process  $e(k_1)h(P_1) \rightarrow e(k_2)h(P_2)\gamma(q_2)$  is,

$$\frac{d\sigma}{dx dy d|\Delta^2| d\phi d\varphi} = \frac{\alpha^3 xy}{16 \pi^2 Q^2 \sqrt{1 + \epsilon^2}} \left| \frac{\mathcal{T}}{e^3} \right|^2. \quad (6)$$

This cross section depends on the Bjorken variable  $x$ , the squared momentum transfer  $\Delta^2 = (P_2 - P_1)^2$ , the lepton energy fraction  $y = P_1 \cdot q_1 / P_1 \cdot k$ , with  $q_1 = k_1 - k_2$ ,

and, in general, two azimuthal angles. The  $\epsilon \equiv 2x\frac{M}{Q}$ . The amplitude  $\mathcal{T}$  is the sum of the DVCS  $\mathcal{T}_{\text{DVCS}}$  and Bethe-Heitler (BH)  $\mathcal{T}_{\text{BH}}$  amplitudes. The azimuthal angular dependence of each of the three terms is defined

$$\mathcal{T}^2 = |\mathcal{T}_{\text{BH}}|^2 + |\mathcal{T}_{\text{DVCS}}|^2 + \mathcal{I}, \quad (7)$$

where  $\mathcal{I}$  is the interference term. These terms could be presented as finite sums of Fourier harmonics:

$$|\mathcal{T}_{\text{BH}}|^2 = \frac{e^6}{x^2 y^2 (1 + \epsilon^2)^2 \Delta^2 \mathcal{P}_1(\phi) \mathcal{P}_2(\phi)} \left\{ c_0^{\text{BH}} + \sum_{n=1}^2 c_n^{\text{BH}} \cos(n\phi) + s_1^{\text{BH}} \sin(\phi) \right\} \quad (8)$$

$$|\mathcal{T}_{\text{DVCS}}|^2 = \frac{e^6}{y^2 Q^2} \left\{ c_0^{\text{DVCS}} + \sum_{n=1}^2 \left[ c_n^{\text{DVCS}} \cos(n\phi) + s_n^{\text{DVCS}} \sin(n\phi) \right] \right\}, \quad (9)$$

$$\mathcal{I} = \frac{\pm e^6}{xy^3 \Delta^2 \mathcal{P}_1(\phi) \mathcal{P}_2(\phi)} \left\{ c_0^{\mathcal{I}} + \sum_{n=1}^3 \left[ c_n^{\mathcal{I}} \cos(n\phi) + s_n^{\mathcal{I}} \sin(n\phi) \right] \right\}, \quad (10)$$

The cross section for a polarized target is given:

$$d\sigma = d\sigma_{\text{unp}} + \cos(\theta) d\sigma_{\text{LP}}(\Lambda) + \sin(\theta) d\sigma_{\text{TP}}(\varphi), \quad (11)$$

where the polar angle  $\theta$  appears in the decomposition of the spin vector  $S = \cos(\theta)S_{\text{LP}}(\Lambda) + \sin(\theta)S_{\perp}(\Phi)$ . The same decomposition was used for the Fourier coefficients.

The four Compton form factors (CFFs),  $\mathcal{H}, \mathcal{E}, \widetilde{\mathcal{H}}, \widetilde{\mathcal{E}}$  directly accessible from the experiment are given by a convolution of perturbatively calculable coefficient functions and corresponding twist-two GPDs [56]. Eight observables, namely the first harmonics  $\cos(\phi)$  and  $\sin(\phi)$  of the interference term, are accessible in polarized beam and target experiments. Thus, experiments with both longitudinally and transversely polarized target can measure all eight Fourier coefficients  $c_{1,\Lambda}^{\mathcal{I}}$  and  $s_{1,\Lambda}^{\mathcal{I}}$  and with  $\Lambda = \{\text{unp}, \text{LP}, \text{TP}_x, \text{TP}_y\}$ . Extraction of CFFs using measured azimuthal moments  $c_{1,\Lambda}^{\mathcal{I}}$  and  $s_{1,\Lambda}^{\mathcal{I}}$  is straightforward:

$$\mathcal{H} = \frac{2-x}{(1-x)D} \left\{ \left[ \left( 2-x + \frac{4x^2 M^2}{(2-x)\Delta^2} \right) F_1 + \frac{x^2}{2-x} F_2 \right] \mathcal{C}_{\text{unp}}^{\mathcal{I}} - (F_1 + F_2) \left[ x \mathcal{C}_{\text{LP}}^{\mathcal{I}} + \frac{2x^2 M^2}{(2-x)\Delta^2} (x \mathcal{C}_{\text{LP}}^{\mathcal{I}} - \mathcal{C}_{\text{TP}+}^{\mathcal{I}}) \right] + F_2 \mathcal{C}_{\text{TP}-}^{\mathcal{I}} \right\}, \quad (12)$$

$$\mathcal{E} = \frac{2-x}{(1-x)D} \left\{ \left[ 4 \frac{1-x}{2-x} F_2 - \frac{4M^2 x^2}{(2-x)\Delta^2} F_1 \right] \mathcal{C}_{\text{unp}}^{\mathcal{I}} + \frac{4xM^2}{(2-x)\Delta^2} (F_1 + F_2) \times (x \mathcal{C}_{\text{LP}}^{\mathcal{I}} - \mathcal{C}_{\text{TP}+}^{\mathcal{I}}) + \frac{4M^2}{\Delta^2} F_1 \mathcal{C}_{\text{TP}-}^{\mathcal{I}} \right\}, \quad (13)$$

$$\widetilde{\mathcal{H}} = \frac{2-x}{(1-x)D} \left\{ (2-x) F_1 \mathcal{C}_{\text{LP}}^{\mathcal{I}} - x(F_1 + F_2) \mathcal{C}_{\text{unp}}^{\mathcal{I}} + \left[ \frac{2xM^2}{\Delta^2} F_1 + F_2 \right] \right\}$$

$$\times \left( x\mathcal{C}_{\text{LP}}^{\mathcal{I}} - \mathcal{C}_{\text{TP}+}^{\mathcal{I}} \right) \Big\}, \quad (14)$$

$$\begin{aligned} \tilde{\mathcal{E}} = \frac{2-x}{(1-x)D} \Big\{ \frac{4M^2}{\Delta^2} (F_1 + F_2) \left( x\mathcal{C}_{\text{unp}}^{\mathcal{I}} + \mathcal{C}_{\text{TP}-}^{\mathcal{I}} \right) + \left[ 4\frac{1-x}{x}F_2 - \frac{4xM^2}{\Delta^2}F_1 \right] \mathcal{C}_{\text{LP}}^{\mathcal{I}} \\ - \frac{4(2-x)M^2}{x\Delta^2}F_1\mathcal{C}_{\text{TP}+}^{\mathcal{I}} \Big\}, \end{aligned} \quad (15)$$

where

$$D = 4 \left( F_1^2 - \frac{\Delta^2}{4M^2} F_2^2 \right) \left( 1 - \frac{\Delta_{\text{min}}^2}{\Delta^2} \right).$$

where real and imaginary parts of  $\mathcal{C}_A^{\mathcal{I}}$  are defined by corresponding  $\cos(\phi)$  and  $\sin(\phi)$  moments of the interference term ( $c_{1,A}^{\mathcal{I}}$  and  $s_{1,A}^{\mathcal{I}}$ ). The CFFs  $\tilde{\mathcal{E}}$  and  $\tilde{\mathcal{E}}$  are dominated by azimuthal moments  $s_{1,TP\pm}^{\mathcal{I}}$  and  $c_{1,TP\pm}^{\mathcal{I}}$  accessible only with transversely polarized target.

For a polarized beam and target with all polarization options, the real and imaginary part of all four CFFs in the twist-three sector can be extracted from the interference term alone by projection onto the  $\cos(2\phi)$  and  $\sin(2\phi)$  harmonics and using Eqs. (12-15).

The procedure of extraction of the  $\sin(\phi)$  moment through measurement of SSA with unpolarized and polarized targets ( $A_{UT,LU,UL}^{\sin\phi}$ ) is the same as described for SIDIS single-spin asymmetries. The projection curves for CLAS12 running with a transversely polarized target have been calculated assuming a luminosity of  $5 \times 10^{34} \text{cm}^{-2} \text{s}^{-1}$ , with a  $NH_3$  target polarization of 85% and a dilution factor 0.14, with 2000 hours of data taking and an overall efficiency 50% (see Fig. 8).

**Transverse target DVCS SSA measurements in addition to unpolarized SSA and longitudinally polarized SSA measurements will provide the full set of data needed for the extraction of CFFs and corresponding GPDs.  $A_{UT}$  is especially sensitive to the GPD  $E$ , and as such will constrain any extraction of the angular momentum  $J$ .**

## 4 SSA in hard exclusive meson production

The hard exclusive leptonproduction of a meson  $M$  from a nucleon target  $N$ ,

$$\ell(k_1)N(P_1) \rightarrow \ell'(k_2)N'(P_2)M(q_2) \quad (16)$$

is a promising process to test QCD in exclusive reactions, as well as a means for studies of the properties of nucleon to hadron transitions.

The amplitude for hard exclusive pseudoscalar meson electroproduction off nucleon was calculated in QCD within the leading  $\alpha_s \ln Q^2 / \Lambda_Q^2 CD$  approximation and

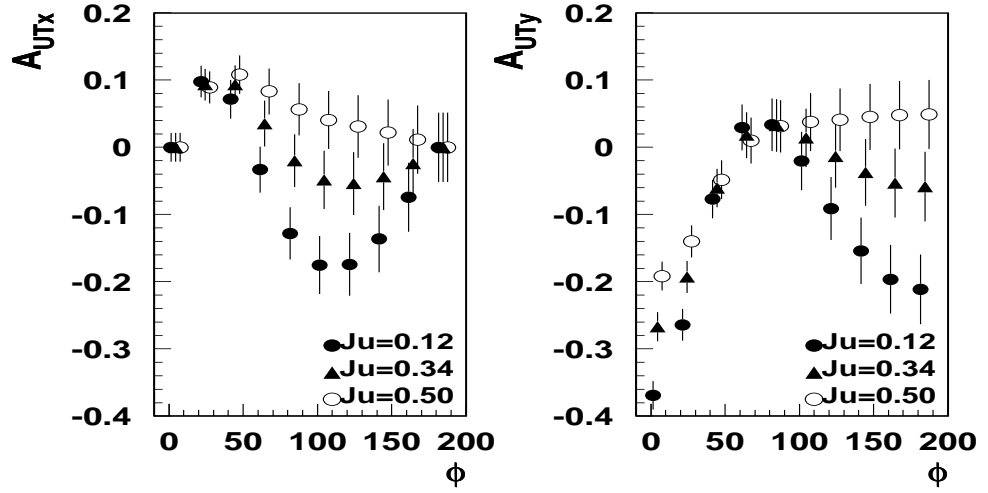


Figure 8: Projected transverse spin asymmetry ( $A_{UT}^{\sin\phi}$ ) in exclusive photon production at 11 GeV. All points correspond to different values of  $J_u$  calculated for the bin with  $\langle t \rangle = 0.5$   $\langle Q^2 \rangle = 2.6$  and  $\langle x \rangle = 0.25$ .

significant transverse spin asymmetries were predicted in distributions of final pions [34]. This dependence is especially sensitive to the pion pole dominated spin flip GPD  $\tilde{E}$ . It was also argued that the scaling for the spin asymmetry sets in at lower  $Q^2$  than that for the absolute cross section. Perturbative next-to-leading order corrections to the hard exclusive leptonproduction of  $\pi^+$  mesons on a transversely polarized proton target were evaluated by Belitsky and Muller [60]. It was shown that corrections can be large and there is a significant scale dependence. Even though for the longitudinal polarization of the virtual photon the amplitude is dominated by twist-two contributions the predictions for the cross section suffer from theoretical uncertainties (see Fig. 9a-b). The theoretical uncertainty in the factorization procedure on the amplitude level is translated into large variations of the physical cross section. However, in the single-spin asymmetry, given by the ratio of the Fourier coefficients of the cross section, the ambiguities approximately cancel. Thus, the perturbative predictions for this quantity are rather stable. The NLO effects result into  $^{+7\%}_{-18\%}$  corrections to the LO prediction for  $0.1 < x < 0.5$ .

The GPD based calculations were performed for the case when the incoming virtual photon is longitudinally polarized. The cross section for the transversely polarized photons is suppressed by a power of  $Q$  [6], but at CLAS energies it may still be significant. Insensitivity to the higher order corrections, is making SSA an appropriate quantity for experimental studies at JLab and will provide an important test of applicability of GPD based predictions at JLab energies.

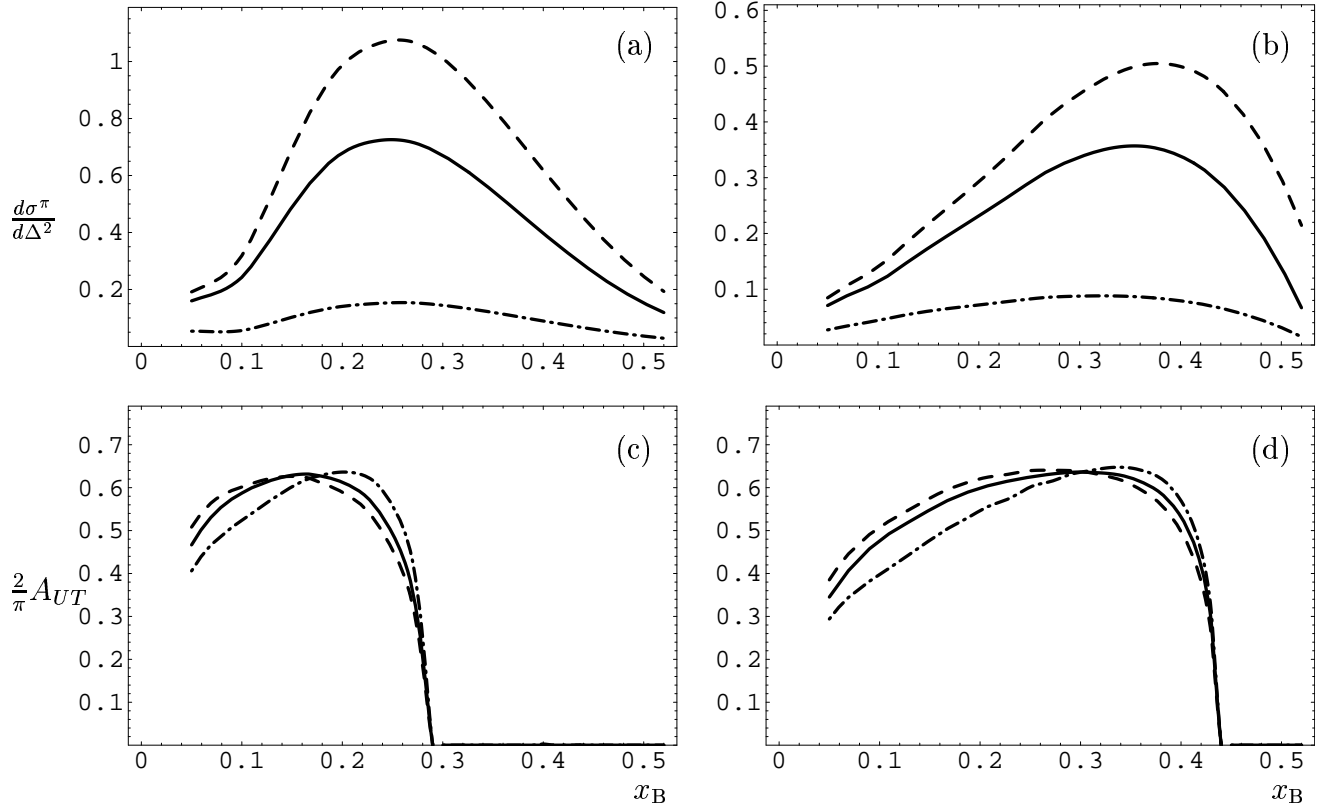


Figure 9: The leading twist predictions for the unpolarized photoproduction cross section  $d\sigma_L^{\pi^+}/d|\Delta^2|$  (in nb/GeV<sup>2</sup>) at  $Q = 10$  GeV<sup>2</sup> [60] are shown for  $\Delta^2 = \Delta_{\min}^2$  and  $\Delta^2 = -0.3$  GeV<sup>2</sup> in the panels (a) and (b), respectively. In (c) and (d) we display the transverse proton single spin asymmetry  $A_{UT}$  for  $\Delta^2 = -0.1$  GeV<sup>2</sup> and  $\Delta^2 = -0.3$  GeV<sup>2</sup>, respectively. The solid, dashed and dash-dotted curves represent the LO and NLO with the naive and BLM scale setting, respectively [60].

Even though the power corrections for the absolute cross section of exclusive meson electroproduction analyzed in terms of generalized parton distributions are expected to be large, there are indications of a *precocious scaling* in ratios of observables [63]. The measurement of spin asymmetries could therefore become a major tool for studying GPDs in the  $Q^2$  domain of a few GeV<sup>2</sup>. Projections for CLAS12 for measurements of transverse asymmetries for vector mesons are shown in Fig. 10. The transverse asymmetries for rhos (neutral and charged) are widely accepted as an important source of independent information on the GPD E. SSA measurements in hard exclusive processes will allow mapping of underlying GPDs and provide access to orbital angular momentum of quarks.

**The data from CLAS transversely polarized target on hard exclusive meson production will provide a test of GPD formalism applicability at CLAS kinematics**

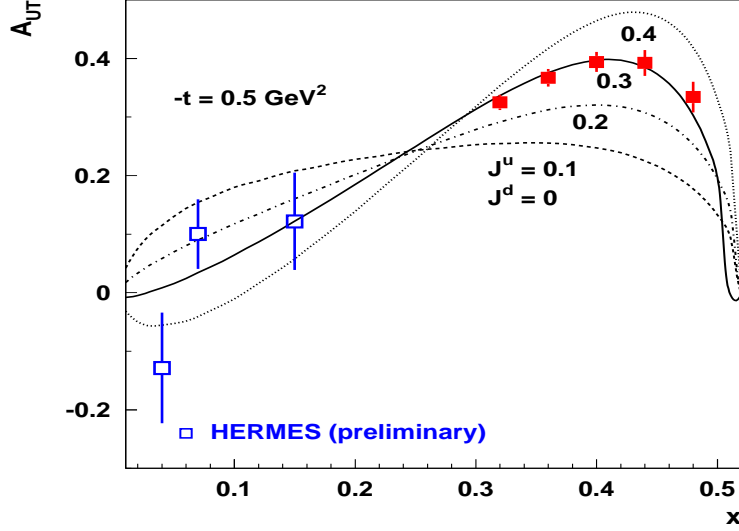


Figure 10: Projections for transverse target asymmetry for exclusive  $\rho^0$  production from hydrogen target (filled squares) using CLAS12 compared to preliminary HERMES data [62].

A key goal of measurements with a transversely polarized target is the simultaneous measurements of the  $Q^2$  and  $x_B$  dependencies of azimuthal moments (SSA) in the cross section of exclusive and semi-inclusive photon (DVCS) and meson electroproduction off the transversely polarized target and extraction of corresponding distribution functions (GPDs,IPDs,TMDs).

## References

- [1] SMC Collaboration (Adeva et al.), Phys. Lett. B 420 (1998) 180.
- [2] HERMES Collaboration (K. Ackerstaff et al.) Phys.Lett. **B464**, 123 (1999).
- [3] EMC Collaboration (Ashman et al.), Phys Lett. B206 (1988) 364.
- [4] X. Ji, Phys. Rev. Lett. **78**, 610 (1997); Phys. Rev. D **55**, 7114 (1997).
- [5] A.V. Radyushkin, Phys. Lett. B **380**, 417 (1996); Phys. Rev. D **56**, 5524 (1997).
- [6] J. C. Collins, L. Frankfurt, and M. Strikman, Phys. Rev. **D56** 2982 (1997).
- [7] P.J. Mulders and R.D. Tangerman, Nucl. Phys. **B461**, 197 (1996).

- [8] A. Kotzinian, Nucl. Phys. **B 441** (1995) 234.
- [9] A. Belitsky,X. Ji and F. Yuan hep-ph/0208038.
- [10] S.Brodsky et.al Phys. Lett. B **530** (2002) 99. hep-ph/0201165.
- [11] J. Collins, hep-ph/0204004.
- [12] X. Ji, F. Yuan e-Print Archive: hep-ph/0206057.
- [13] M. Burkardt, hep-ph/02091179.
- [14] M. Diehl, hep-ph/0205208.
- [15] D.Sivers, Phys.Rev. **D43**, 261 (1991).
- [16] S.Brodsky et.al, hep-ph/0104291
- [17] S.Brodsky et.al, hep-ph/0206259.
- [18] K.Heller et al. 'Proceedings of Spin 96',Amsterdam,Sep.1996,p23
- [19] Fermilab E704 collaboration (A. Bravar et al.), Phys.Rev.Lett. **77**, 2626 (1996).
- [20] Hermes Collaboration (A.Airapetian et al), Phys.Rev.Lett. 87, 182001
- [21] CLAS Collaboration (S.Stepanian et al), Phys.Rev.Lett. 87, 182002
- [22] F.Ellinghaus for the Hermes Collaboration, CIPANP-2006.
- [23] HERMES collaboration (A. Airapetyan et al.), Phys.Rev.Lett. **84**, 4047 (2000).
- [24] HERMES collaboration (A. Airapetyan et al.), Phys.Rev. **D64**, 097101 (2001).
- [25] HERMES collaboration (A. Airapetyan *et al.*), Phys.Rev.Lett. **D64**, 097101 (2004).
- [26] A. Bravar, Nucl. Phys. (Proc. Suppl.) **B79** (1999) 521.
- [27] CLAS Collaboration (H. Avakian et al.) Phys.Rev. D 2003.
- [28] H.Avakian,P.Bosted,V.Burkert,L.Elouadrhiri Proceedings of DIS2005, nucl-ex/0509032.
- [29] P.Bosted et al., CLAS12 proposal to PAC30.
- [30] L.Elouadrhiri et al., The CLAS12 Spectrometer: Components and Performance.
- [31] Efremov et. al hep-ph/0001214,Czech.J.Phys Suppl.



- [32] Bo-Qiang Ma *et al.*, hep-ph/0110324.
- [33] A.Bacchetta et.al Phys.Rev., **D65**, 94021 (2002).
- [34] L. Frankfurt *et al.*, Phys. Rev. D **60** 014010, (1999).
- [35] L. Frankfurt, M. Poliakov, M. Strikman and M. Vanderhaeghen, Phys. Rev. Lett., **84** 2589 (2000).
- [36] A.Miller HERMES Collaboration Proceedings of SPIN2002 BNL,Upton NY 2002.
- [37] COMPASS Collaboration, CERN/SPSLC 96-14.
- [38] R. Seidl, QCD and Hadronic Interactions, La Thuile, Italy, 18-25 Mar 2006, hep-ex/0605085.
- [39] H.Avakian Proceedings of SPIN 2002.
- [40] B. Mecking et al., “The CLAS Detector”, in preparation.
- [41] L. Mankiewicz, A. Schafer and M. Veltri, Comput. Phys. Commun. **71**, 305 (1992).
- [42] J. Ralston and D. Soper, Nucl. Phys. **B152**, 109 (1979)
- [43] R.L.Jaffe and X.Ji Nucl.Phys. **B375** (1992) 527.
- [44] J. Collins, Nucl. Phys. **B396**, 161 (1993).
- [45] M. Anselmino and F. Murgia, Phys. Lett. B **442** (1998) 470.
- [46] A.M. Kotzinian and P.J. Mulders, Phys. Rev. **D 54** (1996) 1229; Phys. Lett. **B406** (1997) 373.
- [47] E. Leader, A. Sidorov and D. Stamenov , Phys.Lett. **B462**,189 (1999).
- [48] H. Kim, M. Polyakov and K. Goike, Phys.Lett. **B387**, 577 (1996).
- [49] D.Boer and P. Mulders, Phys.Rev. **D57**, 5780 (1998).
- [50] A.Efremov K. Goeke, P. Schweitzer Phys.Lett. **B552**, 37 (2001).
- [51] A. M. Kotzinian *et al.*, Nucl.Phys. **A666**, 290-295 (2000).
- [52] A. M. Kotzinian, hep-ph/0504081
- [53] A. M. Kotzinian, B. Parsamyan, A. Prokudin Phys.Rev. **D73**, 114017 (2006); hep-ph/0603194.

- [54] ZEUS collaboration (P.Saull et al.), hep-ex/0003030.
- [55] H1 collaboration (C.Adloff et al.), Phys.Lett. B 517 47, (2001).
- [56] A.Belitsky et al. Nucl.Phys.B629:323-392,2002 hep-ph/0112108.
- [57] CLAS collaboration, S.Chen et al., hep-ex/0605012.
- [58] HERMES collaboration, in preparation.
- [59] HERMES collaboration, in preparation.
- [60] A.Belitsky and D. Muller, Phys.Lett.B513:349-360,2001, hep-ph/0105046
- [61] HERMES Collaboration (Airapetian et al.) Phys.Lett.B535:85-92,2002
- [62] HERMES Collaboration, A. Vandenbroucke, DIS2005 proceedings (2005).
- [63] A. Belitsky hep-ph/0307256.